

LaNi_{1-x}Co_xO_{3-δ} (x=0.4 to 0.7) cathodes for solid oxide fuel cells by infiltration

Aleksander Chrzan^{1,3}, Simona Ovtar², Ming Chen²

¹ Faculty of Electronics, Telecommunications and Informatics, Gdansk University of Technology, Narutowicza 11/12, 80-233 Gdansk, Poland

² Department of Energy Conversion and Storage, Technical University of Denmark, Risø Campus, Frederiksborgvej 399, DK-4000 Roskilde, Denmark

E-mail: aleksander.chrzan@eti.pg.gda.pl

Abstract. Performance of LaNi_{1-x}Co_xO_{3-δ} (LNC) (x=0.4 to 0.7) as a cathode in solid oxide fuel cell (SOFC) is evaluated. Symmetrical cathode/electrolyte/cathode cells for electrochemical testing are prepared by infiltration of yttria stabilized zirconia (YSZ) backbone with LNC solutions. It is showed that the cathode infiltrated with LaNi_{0.5}Co_{0.5}O_{3-δ} (LNC155) has the lowest polarization resistance and activation energy, 197 mΩ cm² at 600 °C and 0.91 eV, respectively. Therefore it is the most promising material of the LNC group for electrochemical applications. X-ray diffraction analysis revealed that none of the materials is single-phased after heat treatment at 800 °C as they contain residues of La₂O₃ and La₂NiO_{4-δ}.

1. Introduction

Solid oxide fuel cells (SOFCs) are electrochemical devices, which when operated above 600 °C efficiently generate electricity. They can utilize hydrogen, biogas or other fuels. Relatively high operating temperature is required for a sufficient catalytic activity of electrodes and an electrolyte ionic conductivity. This causes major problems with mechanical durability, diffusion of cell components and elevates cost of fuel cell stacks fabrication. As a result, there is still ongoing research to improve the catalytic activity and the conductivity of the fuel cells that would reduce the operating temperature [1]. High research focus is on seeking for new, more efficient, more stable or low cost SOFC materials [2]. On the other hand the additional improvement of already existing materials, by varying its microstructure (e.g., producing improved cathode/electrolyte interface) is often reported [3, 4]. One of the ways to alter the structure and improve the properties of electrodes is to increase the surface area available for an electrode reaction. Nano particles have by definition high surface area and consequently high catalytic activity. The efficient way to introduce nano particles into the electrode is by infiltration process. During the infiltration porous, cathode backbone, most commonly made of electrolyte material, is partially filled with a cathode material of choice. The cathode material can be introduced both as suspension or solution [5]. In the case of solution final size and phase composition depends heavily on the heat treatment temperature. Another advantage of using infiltration process is an easy matching of thermal expansion coefficients (TEC) of different layers of SOFC. Since the backbone usually has the same TEC as the rest of the cell, the infiltrated cathode material of very different TEC does not cause



an accelerated delamination. This enables usage of materials with higher TEC like $\text{LaSr}_{1-x}\text{Co}_x\text{O}_{3-\delta}$, $\text{LaNi}_{1-x}\text{Co}_x\text{O}_{3-\delta}$ (LNC) or $\text{LaCoO}_{3-\delta}$ [6, 7].

In this study we report the infiltration of yttria stabilized zirconia (YSZ) backbones with solutions of lanthanum, cobalt and nickel nitrates. LNC was chosen because of its high conductivity and stability in used temperature range [8]. The ratio of Ni to Co was varied from 4:6 to 7:3 to investigate the influence of the chemical composition on the electrochemical performance of symmetrical cells. Different reports about LCN show that the conductivity of compound varies with Ni to Co ratio, as is listed in table 1 [9-10]. The highest conductivity was reported for the compound with Ni:Co ratio of 6:4.

Table 1. Conductivity and thermal expansion coefficient of LNC in literature [9, 10].

composition	σ_{roomT} [Scm^{-1}]	α [10^{-6} K^{-1}]
LN		10
LNC191	170	
LNC182	250	
LNC173	970	
LNC164	1460	14.3
LNC155	1090	
LNC146	700	15.9
LNC137	320	
LNC128	150	
LNC119	40	
LC		22

2. Experimental

For the electrochemical impedance spectroscopy symmetrical cathode/electrolyte/cathode cells were prepared. The chosen LNC compositions were: LNC164, LNC155, LNC146 and LNC137. Cells consisted of 100 μm thick dense YSZ layer and of 47 μm thick porous YSZ backbones on both sides. Backbones porosity was 64% with the pore size between 2 to 4 μm . The cells were prepared by co-sintering of dense and porous tape casted tapes. Further detail on cell fabrication is described elsewhere [11]. Aqueous nitrate solutions of 20% gadolinium doped ceria (CGO) and LNC, containing different Ni:Co ratios were used for infiltration [12]. First, the backbones were infiltrated with CGO precursor solution to prevent reaction between YSZ and LNC. After that backbones were infiltrated with the LNC precursor solution. Each infiltration was followed by firing at 350 $^{\circ}\text{C}$. The number of LNC infiltrations was fixed to nine. Increase of mass of the cathode material in the backbone was followed by weighing samples during the process. Platinum current collector layer was applied on the top of infiltrated cathodes and dried. Finally, the symmetrical cells with infiltrated materials were in-situ heat treated at 800 $^{\circ}\text{C}$ for 2h in an electrochemical setup.

SEM characterization of studied symmetrical cells was performed using Zeiss Supra 35 microscope. HT-XRD was carried out using Bruker D8 with MRI high temperature stage and PSD Lynx Eye detector. XRD spectra were obtained at 800 $^{\circ}\text{C}$ in air using dried LNC solutions. Electrochemical impedance spectra of the symmetrical cells were recorded using Hioki 3522 analyzer with a frequency range from 100 kHz to 1 Hz and an amplitude of 50 mV under the open-circuit conditions. The impedance spectra were measured from 800 $^{\circ}\text{C}$ to 400 $^{\circ}\text{C}$ immediately after the heat treatment. The data were corrected for the series inductance of the measurement rig which was in the range of 85–110 nH. Measurements were analyzed in ZSimpWin software to extract the series and polarization resistance.

3. Results and discussion

Figure 1 shows how the percentage of LNC mass in the total cathode mass was increasing with each infiltration step. It can be seen that the increase of infiltrated material is approximately linear, which means that pores of the backbone were not completely filled with LNC.

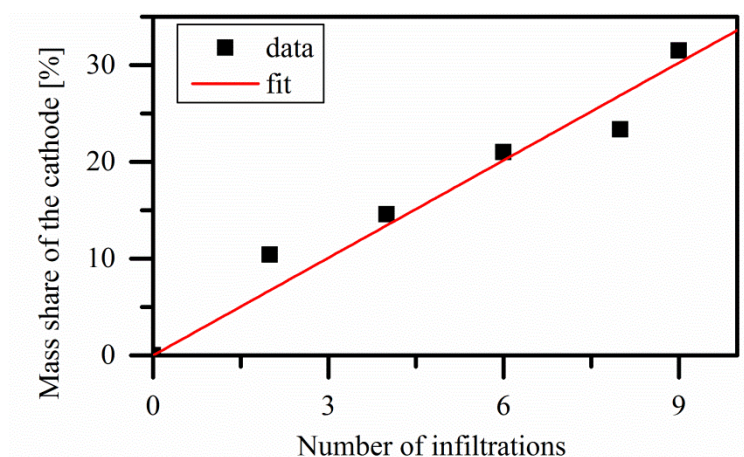


Figure 1. Average mass content of LNC in the cathode during the infiltration process.

Detailed view of the cathodes structure can be seen in figure 2. Figure 2a shows structure of LNC146 infiltrated cathode before measurement. Particles size of the infiltrated material is below the observation limit of used SEM. The infiltrated material seems to cover the whole surface of YSZ grains. Normally well defined YSZ grain boundaries are barely visible after the infiltration. Figure 2b shows the same type of structure after heat treatment at 850 °C. LNC creates porous layer over the YSZ backbone, with the particles size around 70-200 nm.

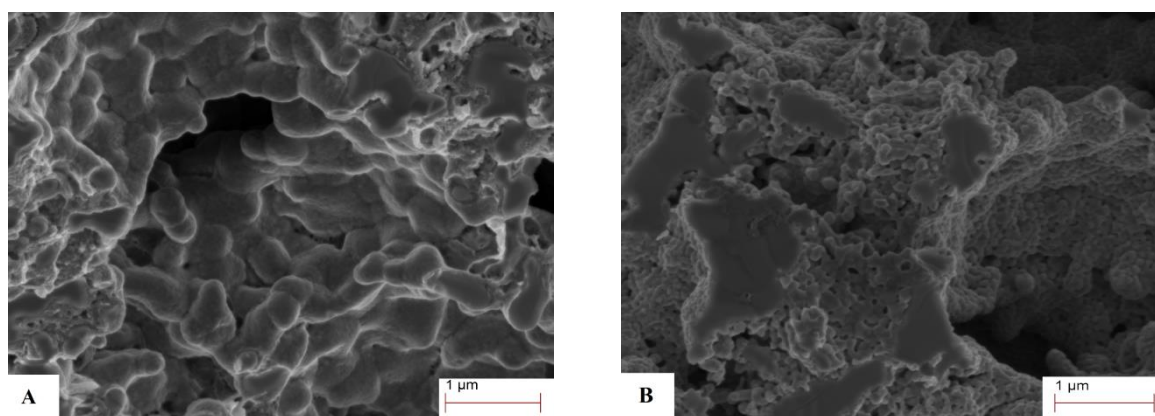


Figure 2. SEM images of the LNC infiltrated symmetrical cell before (A) and after (B) heat treatment.

Dried solutions were investigated using XRD analysis. Figure 3 shows XRD patterns of all 4 LNC materials heated in situ to 800 °C on Pt sample holder. The major phase in all samples is $\text{LaNi}_{1-x}\text{Co}_x\text{O}_{3-\delta}$. As secondary phase La_2O_3 was detected in all samples. With comparing surface area of peaks of LNC phase to La_2O_3 phase, it can be seen that the amount of La_2O_3 slightly varies with Co:Ni ratio in precursor solution. Higher amount of La_2O_3 can be found in LNC146 and LNC164 than in LNC137 and LNC155. In XRD spectra of LNC155 an additional secondary phase of $\text{La}_2\text{NiO}_{4+\delta}$ was observed. The presence of $\text{La}_2\text{NiO}_{4+\delta}$ phase in other samples cannot be excluded, due to detection limit of XRD. To conclude, none

of the materials forms a pure perovskite phase at 800 °C. However, most probably due to homogeneous distribution of phases in backbone there is no evidence that it has an adverse effect on the cathodes performance.

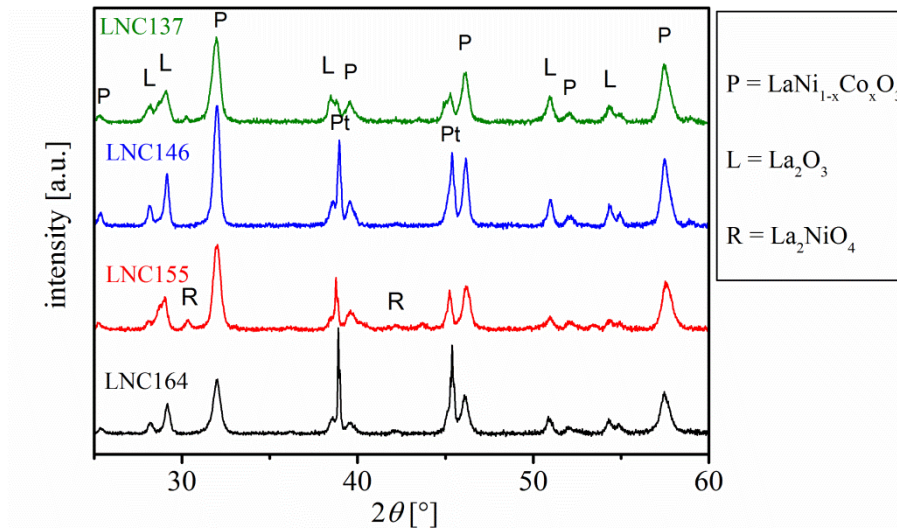


Figure 3. XRD patterns of from the top: LNC137, LNC146, LNC155 and LNC164, obtained at 800 °C.

Impedance spectroscopy performed on the symmetrical cells enabled extraction of a polarization resistance and a series resistance. Typical spectrum measured at 600 °C is shown in figure 4. The polarization resistance results from the electrochemical reactions on the cathode/electrolyte interface. After multiplying with the cathodes surface area and dividing by 2 (due to symmetrical configuration of cell) it is denoted as an area specific resistance (ASR [$\Omega \text{ cm}^2$]) and used to compare the cathodes electrochemical effectiveness. The series resistance almost exclusively results from electrolyte's bulk resistance and, at lower temperatures, grain boundaries resistance. It may be however influenced by the cathode's electronic conductivity and its contact area with the electrolyte. Therefore, in this paper we denote conductivity calculated from the series resistance as “apparent electrolyte conductivity” $\sigma_{el'app}$ to show how effective the cathode is in the distribution of electric current.

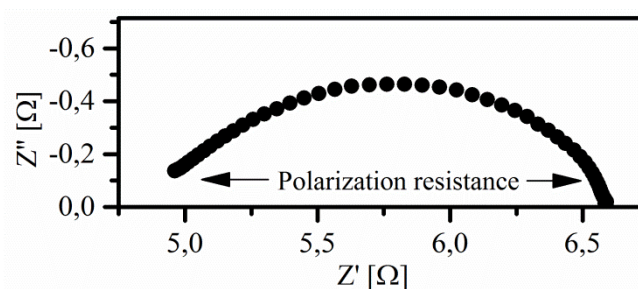


Figure 4. Typical impedance spectrum measured at 600 °C.

Arrhenius plots of ASR are shown in figure 5. Data was fitted with equation (1). It can be noticed that LNC155 is superior at all temperatures except at 700 °C. At 700 °C LNC137 seems to have the lowest ASR , 53 $\text{m}\Omega \text{ cm}^2$ compared to 62 $\text{m}\Omega \text{ cm}^2$ of LNC155.

$$ASR = 1/T A \exp(E_a/kT) \quad (1)$$

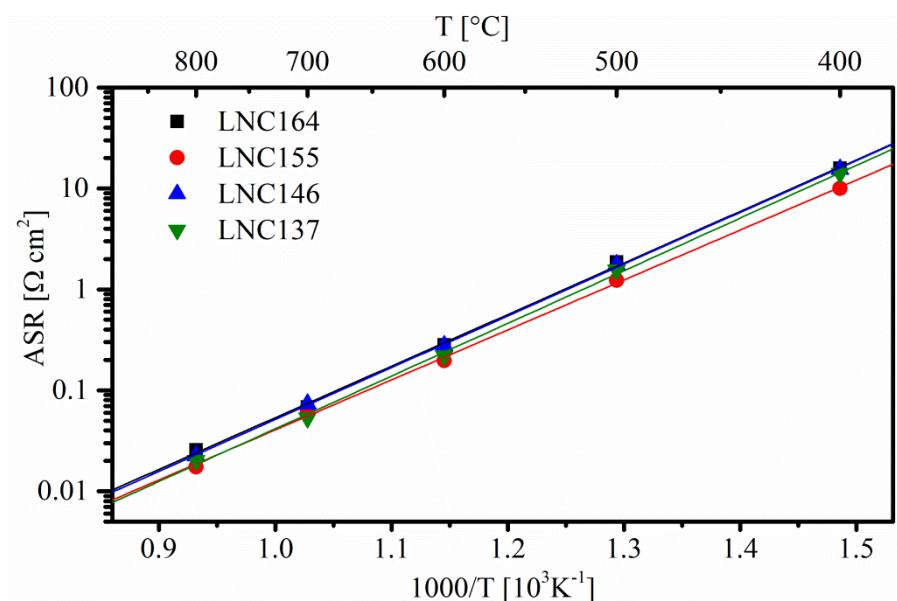


Figure 5. Arrhenius plot of the ASR for the symmetrical cells infiltrated with LNC164, LNC155, LNC146 and LNC137 and in situ sintered at 800 °C.

Table 2 contains parameters calculated from EIS spectra. It can be noticed that LNC137 provides the best current distribution over the electrolyte, since the sample had the highest $\sigma_{el'app}$. It may be connected to the relatively lower amount of La_2O_3 detected in the XRD analysis. However, it is LNC155 that shows the lowest ASR of all, which is especially visible at intermediate temperatures, i.e. 600 °C. LNC155 has also the lowest activation energy, 0.91 eV, while the rest of samples have the average activation energy of 0.95 eV. This may be due to the fact, that this composition is the only one to exhibit a detectable amount of $La_2NiO_{4+\delta}$ phase in XRD analysis, which is a popular catalyst for SOFCs [13]. The ASR for here reported cells is lower than measured for LNC146-CGO composite [14], but is higher than reported for LSC infiltrated into CGO backbone and heat treated at 600 °C [6].

Table 2. Apparent electrolyte conductivity at 800 °C, ASR at 600 °C and 800 °C and ASR activation energy calculated from EIS spectra.

	$\sigma_{el'app}$ at 800 °C [mS cm ⁻¹]	$ASR_{600\text{ °C}}$ [mΩ cm ²]	$ASR_{800\text{ °C}}$ [mΩ cm ²]	$E_{A,ASR}$ [eV]
LNC164	52	282	26	0.94±0.02
LNC155	51	197	17	0.91±0.02
LNC146	54	277	22	0.95±0.01
LNC137	67	219	20	0.96±0.02
LNC146-CGO [14]		440		
LSC-CGO [6]		62		0.87

4. Conclusion

Symmetrical cells infiltrated with $LaNi_{x-1}Co_xO_{3-\delta}$ ($x=0.4$ to 0.7) were tested. Samples infiltrated with LNC155 showed the lowest ASR (17 mΩ cm² at 800 °C) and the lowest ASR activation energy (0.91 eV). XRD analysis revealed that after sintering at 800 °C in all investigated samples secondary phases are present, with the highest amount of La_2O_3 . From the electrochemical performance (low ASR

and activation energy) we can conclude that LNC155 is the most promising infiltration material in LNC series for SOFC applications.

5. References

- [1] Sharaf O Z and Orhan M F 2014 *Renew. Sustainable Energy Rev.* **32** 810-53
- [2] Mahato N, Benerjee A, Gupta A, Omar S and Balani K 2015 *Prog. Mater. Sci.* **72** 147-337
- [3] Chrzan A, Karczewski J, Gazda M, Szymczewska D and Jasinski P 2015 *J. Solid State Electrochem.* **19** 1807-15
- [4] Shah M and Barnett S A 2008 *Solid State Ionics* **179** 2059-64
- [5] Huang Y, Vohs J M and Gorte R J 2006 *Electrochem. Solid State Lett.* **9** A237-40
- [6] Samson A J, Søgard M, Hjalmarsson P, Hjelm J, Bonanos N, Foghmoes S P V and Ramos T 2012 *Fuel Cells* **4** 511-9
- [7] Kiebach R, Knöfel C, Bozza F, Klemensø T, Chatzichristodoulou C 2013 *J. Power Sources* **228** 170-7
- [8] Tsipis E V and Kharton V 2008 *J. Solid State Electrochem.* **12** 1367-91
- [9] Huang K, Lee H Y and Goodenough J B 1998 *J. Electrochem. Soc.* **145** 3220-7
- [10] Hrovat M, Katsarakis N, Reichmann K, Bernik S, Kuščer D and Holc J 1996 *Solid State Ionics* **83** 99-105
- [11] Samson A, Søgard M, Knibbe R and Bonanos N 2011 *J. Electrochem. Soc.* **158** B650-9
- [12] Klemensø T, Chatzichristodoulou C, Nielsen J, Bozza F, Thydén K, Kiebach R and Ramousse S 2012 *Solid State Ionics* **224** 21-31
- [13] Zhang X, Zhang H and Liu X 2015 *J. Power Sources* **269** 412-7
- [14] Hjalmarsson P and Mogensen M 2011 *J. Power Sources* **196** 7237-44

Acknowledgements

The projects ForskeL 2015-1-12276 "Towards Solid Oxide Electrolysis Plants in 2020" funded by Danish Energinet.dk and OPUS DEC-2012/05/B/ST7/02153 "Functional layers for solid oxide fuel cells" funded by National Science Centre Poland are greatly acknowledged. Aleksander Chrzan acknowledges mobility support to DTU from the project POKL.04.01.01-00-368/09: "InterPhD: The development of interdisciplinary doctoral studies at the Gdansk University of Technology in modern technologies".